ISHAM INTERNATIONAL SOCIETY FOR HUMAN AND ANIMAL MYCOLOGY

Medical Mycology, 2014, 52, 293–302
doi: 10.1093/mmy/myt011
Advance Access Publication Date: 13 February 2014
Original Article

Original Article

IFN-γ impairs *Trichophyton rubrum* proliferation in a murine model of dermatophytosis through the production of IL-1β and reactive oxygen species

Ludmila de Matos Baltazar[1], Patrícia Campi Santos[1], Talles Prosperi de Paula[1], Milene Alvarenga Rachid[2], Patrícia Silva Cisalpino[1], Danielle Glória Souza[1] and Daniel Assis Santos[1,*]

[1]Departamento de Microbiologia, Instituto de Ciências Biológicas, Universidade Federal de Minas Gerais, Belo Horizonte Minas Gerais and [2]Departamento de Patologia Geral, Laboratório de Apoptose, Instituto de Ciências Biológicas, Universidade Federal de Minas Gerais, Belo Horizonte Minas Gerais, Brazil

*To whom correspondence should be addressed. Daniel Assis Santos, Departamento de Microbiologia, Instituto de Ciências Biológicas, Universidade Federal de Minas Gerais, Av Antônio Carlos 6627, CEP: 31260-901, Belo Horizonte Minas Gerais. Brazil. Tel: +55 31 3409 2758; Fax: +55 31 3409 2730; E-mail: das@ufmg.br

Received 6 May 2013; Revised 17 July 2013; Accepted 6 September 2013

Abstract

Trichophyton rubrum is the main etiological agent of dermatophytosis, an infection of the skin that affects millions of people worldwide. In this study, we developed a murine model of the dermatophytosis caused by *T. rubrum* in which C57BL/6 wild-type, interleukin (IL)-12$^{-/-}$, and interferon-gamma (IFN-$\gamma^{-/-}$) mice were inoculated with 1×10^6 conidia/animal. The fungal burden, myeloperoxidase and N-acetylglucosaminidase activities, cytokine and chemokine profiles, and histopathology of the skin were evaluated on the seventh and fourteenth days post infection. Phagocytic indices, intracellular proliferation rates, and oxidative bursts generated by macrophages from WT and IFN-$\gamma^{-/-}$ mice were determined. On day 7 post infection, higher fungal burdens were observed comparison with burdens on day 14 post infection. The IL-12$^{-/-}$ and IFN-$\gamma^{-/-}$ mice showed higher fungal burdens on the skin and lower levels of IL-1β. Conversely, the WT mice showed lower fungal burdens with higher production of TNF-α, IL-1β, and chemokine ligand 1/keratinocyte chemoattractant (CXCL1/KC). The macrophages from WT mice proved to be more efficient at engulfing and killing *T. rubrum* conidia through the production of reactive oxygen species. The results show that our model is a useful tool for understanding the pathogenesis of dermatophytosis caused by *T. rubrum* and that IL-12 and IFN-γ are pivotal in controlling the infection through the recruitment and activation of neutrophils and macrophages.

Key words: dermatophytosis, *T. rubrum*, IFN-γ, IL-1β.

Introduction

Dermatophytes are filamentous fungi that cause infection in keratinized tissues such as skin, nails, and hair [1,2]. The species of this group are classified as geophilic, zoophilic, and anthropophilic fungi according to their habitat. Although species of all three of these groups can be etiological agents of human disease, infections caused by the anthropophilic species are more common, and *Trichophyton rubrum* is the most prevalent etiologic agent worldwide [3]. Typically, *T. rubrum* develops cottony white colonies with clavate microconidia and a blood-red color on the reverse side on Sabouraud glucose agar and potato dextrose agar (PDA) [1].

The kinetics of infection by this fungus involves colonization of the stratum corneum by hyphae growing in multiple directions [4]. After establishment of the infection, its clinical aspects are variable and are the result of a combination of keratin destruction with inflammatory response of the host [1,2]. Usually, the dermatophytosis classification is performed considering the anatomic site of infection, that is, infection of glabrous skin (tinea corporis, tinea cruris, and tinea faciei), infection of keratinized area (tinea manuum and tinea pedis), infection of hair follicles (tinea capitis and tinea barbae), and nail infections (tinea unguium) [1,2]. Although less common, severe manifestations such as infection of dermal and subcutaneous tissues and the generation of a granulomatous inflammation named Majocchi's granuloma, invasive disease, and disseminated infection in immunocompromised patients could occur [5–9].

It has been widely suggested that the host inflammatory response to fungal infection involves the production of interleukin (IL)-12 and the participation of interferon-gamma (IFN-γ)–producing T cells [10–14]. However, the pathway involving IL-12 and IFN-γ in dermatophytosis is still unknown, mainly due to the lack of a reliable experimental model for the disease caused by *T. rubrum*. IL-12 and IL-18 regulate the production of IFN-γ, which is a proinflammatory cytokine involved in the generation of reactive oxygen species (ROS) by macrophages, neutrophils, and dendritic cells [15]. In addition, IL-1β has been shown to be an important cytokine for the control of fungal infection [16], as it is also an important proinflammatory mediator whose production is controlled by multiprotein complexes called inflammasomes [17,18]. Despite this knowledge about the participation of IL-1β in containing infection by different fungi, its role in controlling the infection by *T. rubrum* remains unclear.

The animal models of dermatophytosis have focused primarily on zoophilic species, and studies of anthropophilic species such as *T. rubrum* are scarce. Although models in which the fungus is cultivated *in vitro* on keratinized surfaces (such as nails and skin fragments) or in cultures of keratinized tissue have been developed, these models are only able to determine the ability of *T. rubrum* to grow on different substrates, and they fail to characterize the global host response during infection [19–21]. Animal models of the infection caused by *T. rubrum* would be useful for studying the host–fungus interaction in order to provide new insights into the immune response triggered by dermatophytosis and to test the efficacy of new antifungal drugs. The aim of this study was to develop a murine model of *T. rubrum* dermatophytosis and evaluate the roles of IL-12 and IFN-γ in the disease. The results suggest that the pathway by which IL-12 regulates IFN-γ production is important for reducing the fungal burden through promotion of the production of IL-1β and host oxidative burst.

Materials and methods

Ethical statements

The Committee on the Ethics of Animals Experiments of the Universidade Federal de Minas Gerais (CEUA/UFMG, protocol n° 029/2009) approved all protocols. All experiments were performed under ketamine/xylazine (80/15 mg/kg) anesthesia administered intraperitoneally.

Mice

Wild-type (WT) C57BL/6 mice and mice deficient for IFN-γ (IFN-$\gamma^{-/-}$) or interleukin-12p40 (IL-12$^{-/-}$) were bred and maintained at the Instituto de Ciências Biológicas, Universidade Federal de Minas Gerais, Brazil. For all experiments, male 6- to 8-week-old mice were kept in a controlled environment in filtered cages with *ad libitum* access to autoclaved food and water.

Trichophyton rubrum strain and inoculum preparation

All experiments were performed using the reference strain *T. rubrum* ATCC (American Type Culture Collection) 28189 (Instituto Nacional de Controle de Qualidade em Saúde [INCQS] 40051). Seven-day-old colonies on PDA were used for the preparation of inocula. The colonies were covered with 5.0 ml of phosphate-buffered saline (PBS; pH 7.4) and scraped with a sterile platinum loop. After 20 minutes of hyphal sedimentation, the supernatants from the suspensions were counted in a hemocytometer, and animals were inoculated at a final concentration of 1×10^6 microconidia per animal in a maximum volume of 100 µl, as described below. For phagocytosis assays, the suspensions of conidia and hyphae were filtered using a Whatman filter, model 40 (pore size, 8 µm), which retains hyphal fragments

and only permits the passage of *T. rubrum* microconidia [22]. The density of microconidia was determined with a hemocytometer and adjusted to 1×10^6 microconidia/ml.

In vivo challenge

A 2×2 cm^2 area on the backs of WT, IFN-$\gamma^{-/-}$, and IL-$12^{-/-}$ mice was shaved and scarred with a sterile scalpel. Microconidia (1×10^6 cells/animal) were inoculated within both cutaneous and subcutaneous tissues at four points on the shaved area, with a maximum volume of 100 µl per animal. The control mice were inoculated with 100 µl of PBS. The experiments were performed on day 7 and day 14 post infection. The mice were euthanized after ketamine/xylazine (80/15 mg/kg) anesthesia, and the shaved area of skin was collected aseptically for the determination of fungal burden and histopathology and for quantification of myeloperoxidase (MPO) and N-acetylglucosaminidase (NAG) activities as well as cytokine and chemokine levels.

Fungal burden

The fungal burden was determined by macerating the skin with 1.0 ml of sterile PBS. Fifty microliters of the suspension was plated on PDA and incubated at 28°C for 72 hours. The results were expressed as colony-forming units per gram of skin.

Cytokine and chemokine levels on the skin

One hundred milligrams of skin was homogenized in 1.0 ml of PBS supplemented with antiproteases (0.1 mM phenylmethilsulfonyl fluoride, 0.1 mM benzethonium chloride, 10 mM ethylenediaminetetraacetic acid [EDTA], and 20 KI aprotinin A) and 0.05% Tween. The samples were centrifuged at 3000 × g for 10 minutes and the supernatant used for enzyme-linked immunosorbent assay. The cytokines (TNF-α, IFN-γ, IL-12, IL-1β, IL-6, and IL-10) and CXCL1/KC levels on the skin were determined using commercially available antibodies according to manufacturer's instructions (R&B Systems, Minneapolis, MN, USA). The results were expressed as nanograms per gram of tissue.

MPO activity

MPO activity is a quantitative index for measuring the recruitment of neutrophils to tissue [23]. One hundred milligrams of skin was homogenized in 1.9 ml of pH 4.7 buffer (0.1 M NaCl, 0.02 M Na_3PO_4, and 0.015 M Na_2–EDTA) and centrifuged at 78.26× g for 10 minutes. The supernatant was discarded. The remaining pellet was incubated with 1.5 ml of 0.2% NaCl solution; after 30 seconds, 1.5 ml of 1.6% NaCl supplemented with 5% glucose was added. This solution was homogenized and centrifuged at 78.26× g for 10 minutes. The pellet was resuspended in 1.9 ml of buffer containing 0.05 M Na_3PO_4 and 0.5% hexadecyltrimethylammonium bromide and then homogenized. The suspension was submitted to three freeze–thaw steps using liquid nitrogen and centrifuged at 78.26× g for 10 minutes. The supernatant was used to assay the MPO activity in a 96-well microplate where 25 µl of 1.6 M tetramethylbenzidine containing 0.002% H_2O_2 was added to 25 µl of homogenate and incubated for 5 minutes at 37°C. The reaction was stopped by adding 100 µl of 1 M H_2SO_4 and read on a spectrophotometer at 450 nm [23]. The results were expressed as relative units of MPO.

NAG activity

NAG activity is a quantitative index for the measurement of macrophage recruitment to tissue [24]. One hundred milligrams of skin was homogenized in 1.9 ml of pH 4.7 buffer (0.1 M NaCl, 0.02 M Na_3PO_4, and 0.015 M Na_2–EDTA) and centrifuged at 78.26× g for 10 minutes. The pellet was resuspended in 1.5 ml of 0.2% NaCl; after 30 seconds, 1.5 ml of 1.6% NaCl supplemented with 5% glucose was added, and the mixture was homogenized. The suspension was centrifuged at 78.26× g for 10 minutes, and the supernatant was discarded. The pellet was resuspended in 2.0 ml of 0.9% saline containing 0.1% v/v of Triton X-100 at 4°C, homogenized, and centrifuged at 78.26× g for 10 minutes. The supernatant was used to measure the NAG activity using a 96-well microplate. After the addition of 100 µl p-nitrophenyl-N-acetyl-D-glucosaminide (Sigma-Aldrich, St. Louis, MO, USA) dissolved in citrate/phosphate buffer (0.1 M citric acid and 0.1 M Na_2PO_4, pH 4.5) at a final concentration of 2.24 mM, the reaction was stopped by the addition of 100 µl of 0.2 M glycine buffer (pH 10.6) and quantified at 405 nm in a spectrophotometer [24]. The results were expressed as relative units.

Phagocytosis assay

Intraperitoneal macrophages were isolated from 6- to 8-week-old WT and IFN-$\gamma^{-/-}$mice. Briefly, the animals were intraperitoneally treated with 2.0 ml of a 3% thioglycolate (w/v) solution (Himédia; Curitiba, Paraná, Brazil) 5 days before the experiment. The peritoneum was washed with PBS, and the cells were pooled and washed with Roswell Park Memorial Institute (RPMI) 1640 medium buffered with sodium bicarbonate (Himédia) and centrifuged at 78.26× g for 10 minutes. The cells were resuspended in RPMI 1640 medium supplemented with 5% (v/v) fetal calf

serum and gentamicin (Sigma) at 40 mg/ml and buffered with sodium bicarbonate. The concentration of cells was determined using a hemocytometer. The cells were plated at 1×10^6 cells/ml/well in triplicate in 24-well plates with glass coverslips [25]. After 24 hours, the wells were washed and new RPMI 1640 medium containing 1×10^6 conidia/ml was added to each well. The macrophages were incubated with *T. rubrum* conidia for 2, 6, and 12 hours at 37°C and 5% atmospheric CO_2. The glass coverslips were washed with PBS, fixed with acetone, and stained with Panoptic (Renylab, Barbacena, MG, Brazil). The phagocytic index was determined by counting the internalized conidia in at least 100 macrophages [26].

Intracellular proliferation measurement

The intracellular proliferation assay was performed 24 hours after the macrophages were challenged with *T. rubrum* conidia, according to the phagocytosis assay protocol, with cells from WT and IFN-$\gamma^{-/-}$ mice. For this assay, the medium was removed 6 hours after the cells were challenged with *T. rubrum* conidia, and new RPMI 1640 medium supplemented with 5% (v/v) fetal calf serum, 40 mg/ml gentamicin (Sigma), and buffered sodium bicarbonate were added. After 24 hours, each well was washed with PBS, and sterile distilled water was added to lyse the macrophages [27]. Thirty microliters of the resulting suspension was plated in PDA and incubated at 28°C for 72 hours. The results were expressed as the quotient of the colony-forming units/phagoccytic index (cfu/PI).

Evaluation of the intracellular oxidative burst by macrophages challenged with *T. rubrum*

The kinetics of ROS production was evaluated in macrophages from WT and IFN-$\gamma^{-/-}$ mice challenged with *T. rubrum* microconidia as described above. The control groups are represented only by macrophages. The levels of ROS production were measured by treating the samples with 50 μM of 2′,7′dichlorodihydrofluorescein diacetate (Invitrogen, Foster City, CA, USA) [28,29] for 30 minutes at 37 °C and 5% atmospheric CO_2. The fluorescence was determined in a fluorometer (Synergy 2, BIOTEK, Winooski, VT, USA) at a wavelength of 485 nm and a measuring emission of 530 nm. ROS production was measured after the macrophages and fungi were incubated for 2 hours, readings were taken every 20 minutes for 6 hours. The data were expressed as the mean ± standard error of the mean (SEM) for the fold increase of fluorescence over the control.

Histopathology

The skin was removed during necropsy 7 or 14 days post infection and immediately fixed in buffered 10% formalin (v/v). The tissue was embedded in paraffin, and the sections were stained with hematoxylin and eosin (Sigma) and examined under light microscopy.

Statistical analysis

Statistical analyses were performed using the GraphPad Prism software (GraphPad Software, La Jolla, CA, USA) using one-way analysis of variance, Kruskal–Wallis, and Newman–Keuls multiple comparison tests. A P value <0.05 was considered to be significant, and the results are shown as the mean ± SEM.

Results

Characterization of infection by *T. rubrum* in the skin of WT mice

The mice were euthanized on the 7th day and the 14th day post infection (d.p.i.), and the skin was removed for fungal burden assay. Figure 1 shows fungal burdens, with higher levels found on the 7th d.p.i. ($P < 0.05$; Fig. 1A). The MPO levels were higher ($P < 0.0001$) in WT mice on the 7th d.p.i. than in the noninfected (NI) group (Fig. 1B). The NAG activity was higher ($P < 0.0001$) in the WT mice on the 7th and 14th d.p.i. compared with the NI group (Fig. 1C). The histopathology analysis showed normal histological appearance in the NI mice on the 7th (Fig. 1D) and 14th d.p.i. (data not shown). On the 7th d.p.i., the WT mice showed mild dermatitis (asterisks) and epidermal hyperplasia (arrow; Fig. 1E) compared with NI mice. The WT mice on the 14th d.p.i. showed mild infiltration of inflammatory cells in the deep dermis and hypodermis (asterisk; Fig. 1F) compared with the NI group.

IFN-γ is important to impair *T. rubrum* proliferation in the skin of mice

The levels of IL-12 and IFN-γ, fungal burden, and histopathology were evaluated on the 7th and 14th d.p.i. in WT, IL-12$^{-/-}$, and IFN-$\gamma^{-/-}$ mice. Infection with *T. rubrum* was correlated with increased levels of IFN-γ on the 14th d.p.i. in WT mice ($P < 0.0001$) compared with the NI group (Fig. 2A). The IL-12$^{-/-}$ and IFN-$\gamma^{-/-}$ mice presented higher ($P < 0.0001$) fungal burdens than the WT mice on the 7th d.p.i. (Fig. 2B). There were no differences in lesion size among WT, IL-12$^{-/-}$, and IFN-$\gamma^{-/-}$ mice. The histopathology analysis showed an IL-12$^{-/-}$ mouse with mild to moderate dermatitis on the 7th d.p.i. (Fig. 2F)

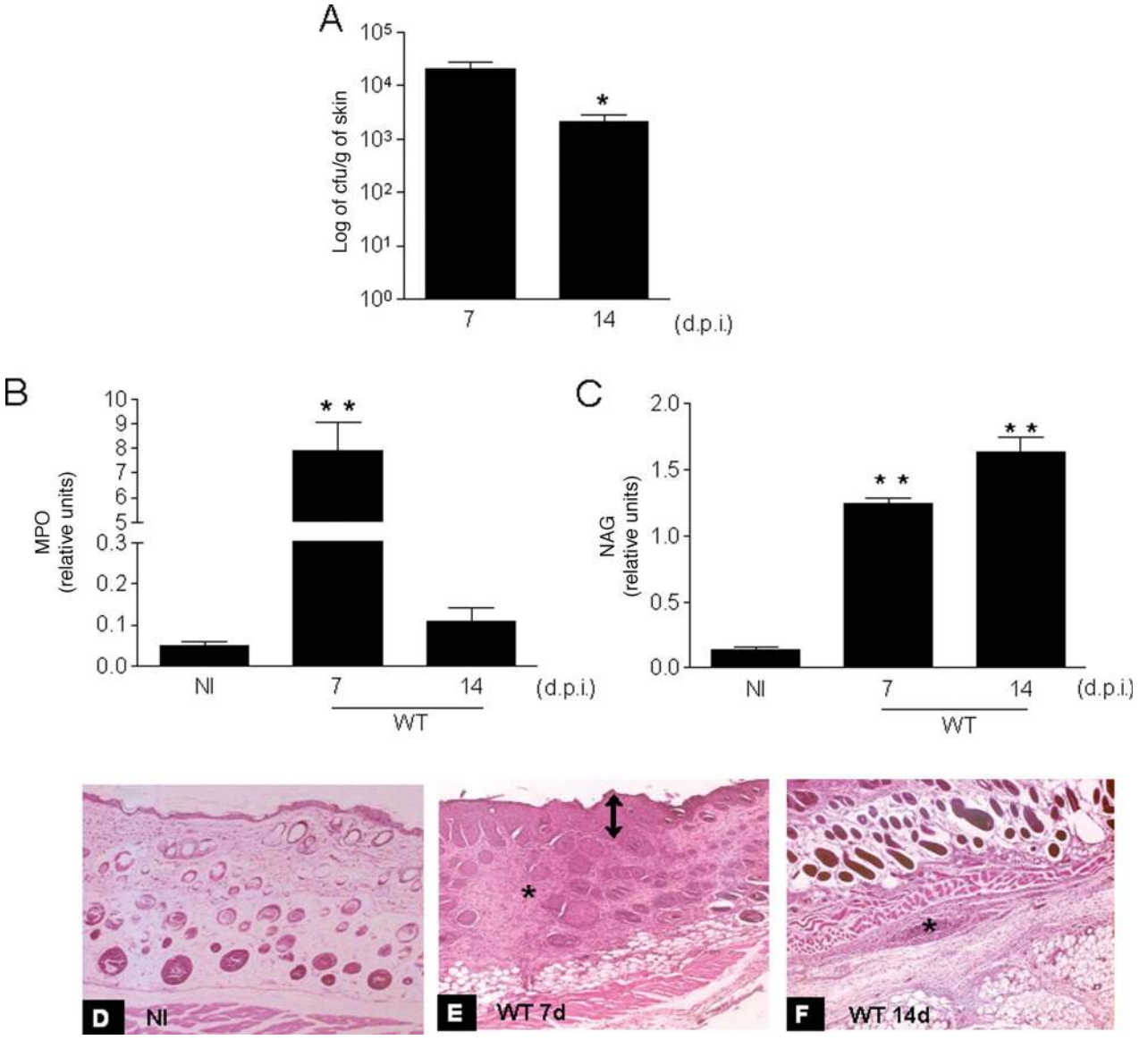

Figure 1. Characterization of *Trichophyton rubrum* infection in C57BL/6 WT mice. The animals were inoculated with 1×10^6 *T. rubrum* conidia/animal, and the fungal burden (cfu/g of skin), MPO and NAG levels, and histopathology assay were evaluated at the indicated time points. (A) Fungal burden on the 7th and 14th d.p.i. (B) MPO activity on the 7th and 14th d.p.i. (C) NAG activity on the 7th and 14th d.p.i. (D) Histopathological analysis of the skin of uninfected animal. (E) Histopathological analysis of the skin of WT mouse on the 7th d.p.i. Mild dermatitis is indicated by asterisks and epidermal hyperplasia by arrow. (F) Histopathological analysis of the skin of WT mouse on the 14th d.p.i. Mild infiltration of inflammatory cells in the deep dermis and hypodermis is indicated by asterisk. Results are expressed as the mean ± SEM. N = 6 mice per group. D–F: ×100. $^{**}P < 0.0001$. $^{*}P < 0.05$. d.p.i., days post infection; NI, noninfected mice; WT, wild type. This Figure is reproduced in color in the online version of *Medical Mycology*.

compared with the NI mouse. On the 14th d.p.i., the IL-$12^{-/-}$ mouse presented with an inflammatory nodule composed of a large central necrotic area mixed with neutrophils and degenerated cells and a thin capsule of connective tissue compared with the NI mouse (Fig. 2G). The IFN-$\gamma^{-/-}$ mouse showed a moderate dermatitis, mild epidermal hyperplasia, and hyperkeratosis on the 7th d.p.i. (Fig. 2H) compared with the NI mouse. The IFN-$\gamma^{-/-}$ mouse showed mild dermatitis on the 14th d.p.i. compared with the NI mouse (Fig. 2I).

Infection with *T. rubrum* induces the production of CXCL1/KC and cytokines related to the recruitment of inflammatory cells to the site of infection

The MPO and NAG activities and the levels of TNF-α, IL-1β, IL-6, IL-10, and CXCL1/KC were evaluated in the skin of the infected mice after the 7th and 14th d.p.i. Figure 3 demonstrates that infection with *T. rubrum* caused the recruitment of immune cells such as neutrophils and macrophages, as shown by the MPO and NAG assay, respectively. The MPO levels were higher ($P < 0.0001$)

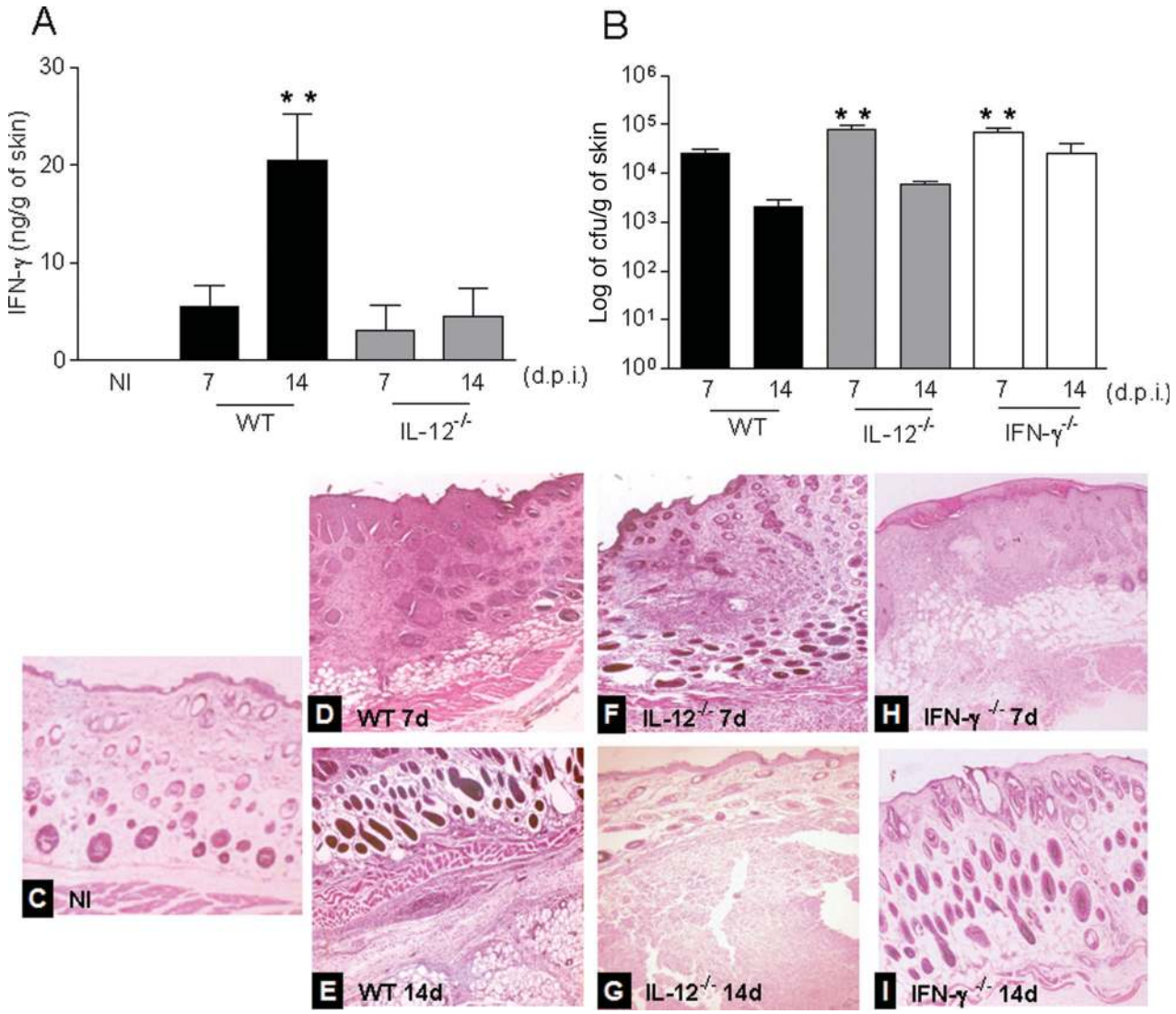

Figure 2. Production of IFN-γ is important for control of the infection. WT, IFN-$\gamma^{-/-}$, and IL-12$^{-/-}$ mice were inoculated with 1×10^6 *Trichophyton rubrum* conidia/animal, and the levels of IL-12 and IFN-γ, fungal burden, and histopathology analysis were evaluated at the indicated time points. (A) Levels of IFN-γ on the 7th and 14th d.p.i. (B) Fungal burden at the 7th and 14th d.p.i. (C) Histopathological analysis of the skin of a NI animal (D) Histopathological analysis of the skin of WT mouse on the 7th d.p.i. (E) Histopathological analysis of the skin of WT mouse on the 14th d.p.i. (F) Histopathological analysis of the skin of IL-12$^{-/-}$ animal on the 7th d.p.i. (G) Histopathological analysis of the skin of IL-12$^{-/-}$ mouse on the 14th d.p.i. (H) Histopathological analysis of the skin of IFN-$\gamma^{-/-}$ animal on the 7th d.p.i. (I) Histopathological analysis of the skin of IFN-$\gamma^{-/-}$ mouse on the 14th d.p.i. Results are expressed as the mean ± SEM. N = 6 mice per group. C–I: ×100. $^{**}P < 0.0001$. $^{*}P < 0.05$. d.p.i., days post infection; NI, noninfected; WT, wild type. This Figure is reproduced in color in the online version of *Medical Mycology*.

in WT mice on the 7th d.p.i. (Fig. 3A) than in the NI group. NAG activity analysis showed that all infected mice presented higher ($P < 0.0001$) macrophage recruitment in comparison with the NI group (Fig. 3B). The mice deficient for the production of IL-12 and IFN-γ presented lower levels of MPO, which were similar to those of the NI group. Increased levels of CXCL1/KC ($P < 0.0001$), IL-1β ($P < 0.0001$), and TNF-α ($P < 0.05$) were observed on the 7th d.p.i. in WT mice (Fig. 3C, D, and E) compared with the NI mice. On the 14th d.p.i., the WT mice showed higher levels ($P < 0.0001$) of IL-1β compared with NI mice (Fig. 3E). There were no differences in IL-6 and IL-10 levels among the groups, and IFN-γ was undetectable in IFN-$\gamma^{-/-}$ mice (data not shown).

Macrophages from WT mice presented PI and higher oxidative burst levels

Analysis of the phagocytosis assay revealed that the PI increased in a time-dependent manner for all groups (Fig. 4A). However, the PIs of macrophages from IFN-$\gamma^{-/-}$ mice

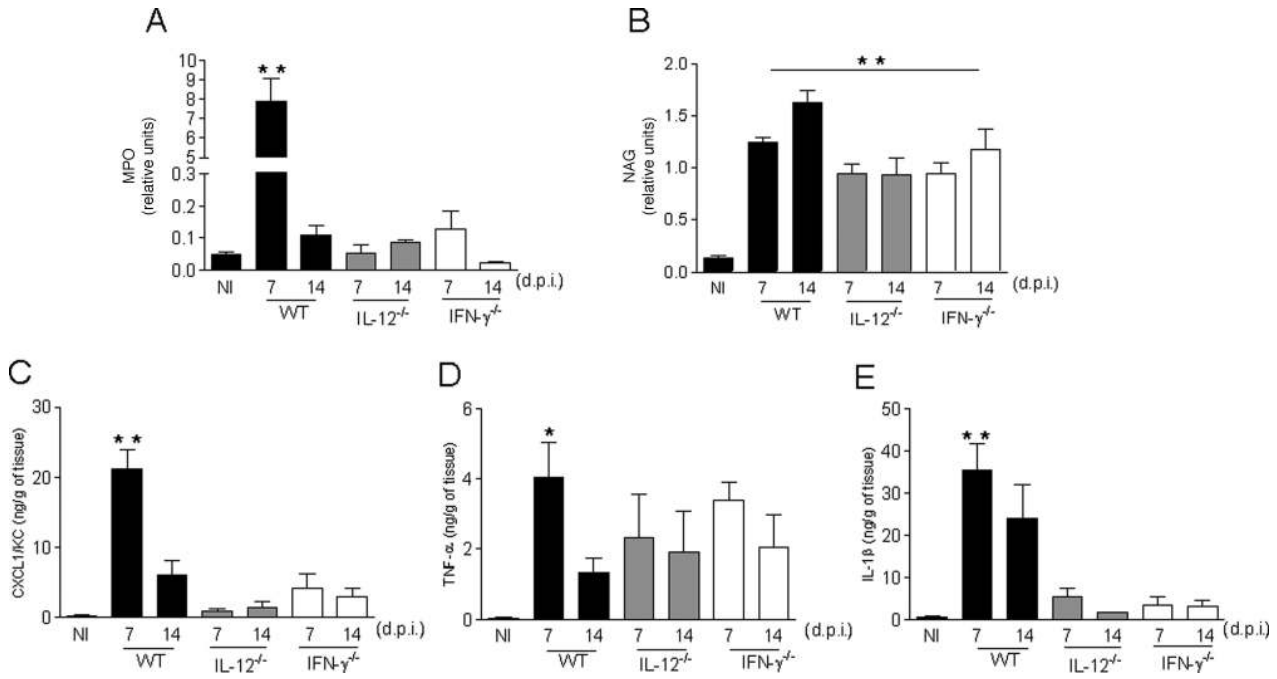

Figure 3. Control of the infection is related to the recruitment of inflammatory cells and CXCL1/KC, TNF-α, and IL-1β production. WT, IFN-$\gamma^{-/-}$, and IL-12$^{-/-}$ animals were used for evaluation of MPO and NAG activities and levels of CXCL1/KC, TNF-α, and IL-1β after day 7 and day 14 with 1×10^6 *Trichophyton rubrum* conidia/animal. (A) MPO activity on the 7th and 14th d.p.i. (B) NAG activity on the 7th and 14th d.p.i. (C) CXCL1/KC levels (ng/g of tissue), (D) TNF-α levels (ng/g of tissue), and (E) IL-1β (ng/g of tissue) on the 7th and 14th d.p.i. Results are expressed as the mean ± SEM. N = 6 mice per group. $^{**}P < 0.0001$. $^{*}P < 0.05$. d.p.i., days post infection; NI, noninfected; WT, wild type.

were lower than those from WT mice ($P < 0.0001$) at all times tested (Fig. 4A). The intracellular proliferation assay showed that the IFN-$\gamma^{-/-}$ group had a higher intracellular proliferation rate (IPR; $P < 0.0001$) than the WT group (Fig. 4B). The kinetics of the production of ROS by WT and IFN-$\gamma^{-/-}$ macrophages showed that cells from WT mice challenged with *T. rubrum* conidia presented higher ($P < 0.0001$) rates of oxidative burst than the control groups (only macrophages from WT and IFN-γ–deficient mice) and the group of macrophages from IFN-$\gamma^{-/-}$ mice challenged with *T. rubrum* conidia (Fig. 4C).

Discussion

The development of a murine model of *T. rubrum* dermatophytosis is a worthwhile strategy because there are several important questions about the immunopathogenesis of the disease that are difficult to address with current models [19,30,31]. Human infection by *T. rubrum* involves the adhesion of arthroconidia on stratum corneum [32], with further connection of these structures to keratinocytes [2]. According to Esquenazi et al. [33], microconidia may also attach to keratinocytes, and this adherence is mediated by carbohydrate-specific adhesion. Furthermore, models using skin fragments have demonstrated that dermatophyte microconidia are able to germinate and cause damage to the tissue [19]. We chose microconidia (instead of arthroconidia or hyphae) to perform the infection because this strategy has been demonstrated to provide more reliability regarding the exact numbers of viable fungi [22]. The infections with microconidia were reproducible, allowing us to obtain similar results when the tests were repeated. In addition, the fact that *T. rubrum* is an anthropophilic fungus would not be considered an impediment to its use in mice because other fungi, including *Paracoccidioides brasiliensis* and *Aspergillus fumigatus*, have been tested in murine models with reliable results. In the latter example, immunocompromised animals were needed to reproduce the disease [34,35].

Infection by dermatophytes generally induces the production of IFN-γ in the skin of patients with dermatophytosis [8,36,37] and in peripheral blood mononuclear cells challenged with trichophytin [38]. In this study, we demonstrated that a deficiency of IL-12 or IFN-γ was related to increased fungal burden in the skin of mice (Fig. 2). Higher levels of IFN-γ expression were demonstrated by both Nakamura et al. [39] in an animal model of contact hypersensitivity and by Venturini et al. [40] in an animal model of dermatophytosis caused by *T. mentagrophytes*. The animal model developed in this study confirms that IL-12 and IFN-γ are essential to containing the infection by

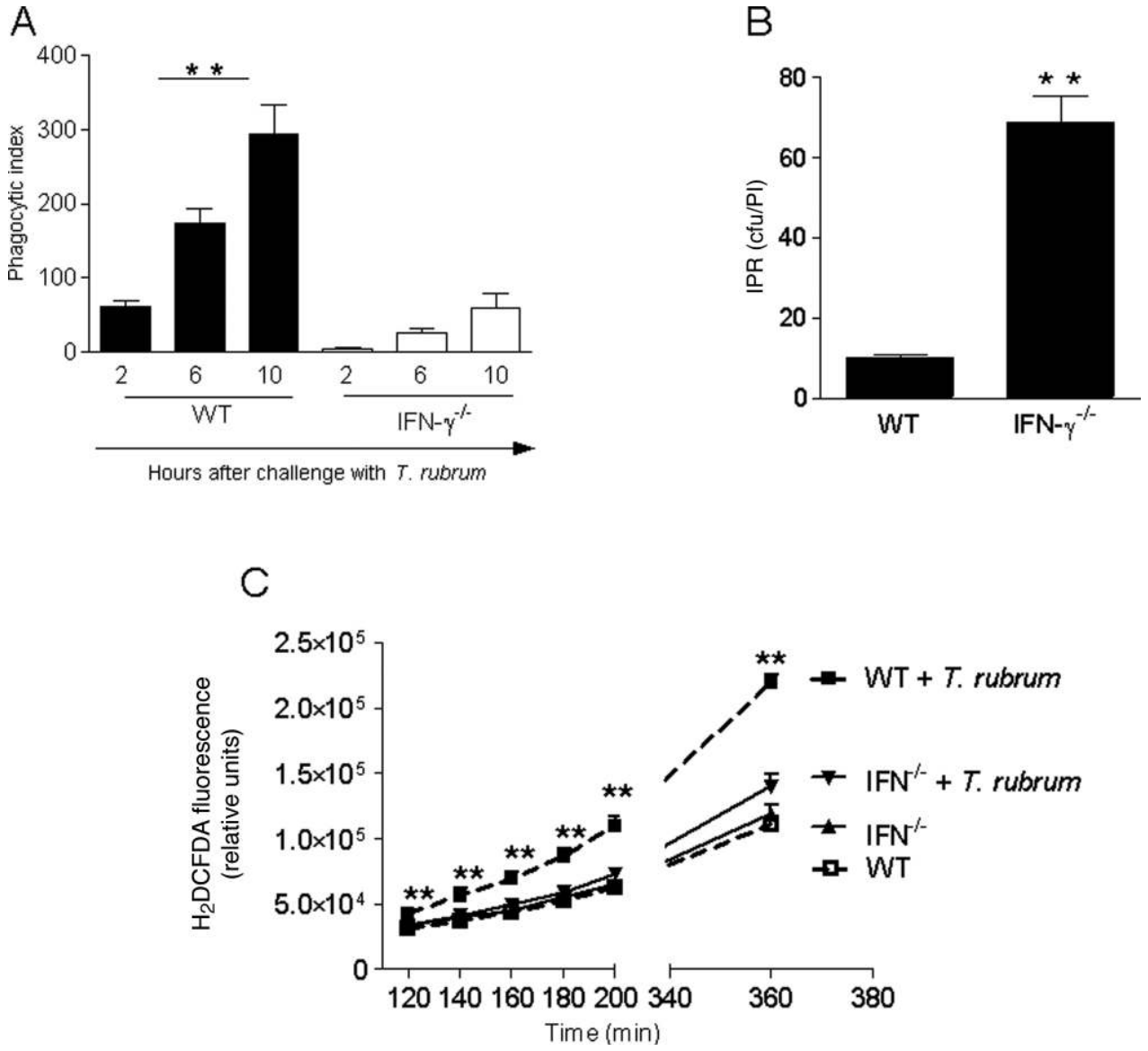

Figure 4. Macrophages from WT mice showed higher PI and ROS production and lower IPR than those from IFN-$\gamma^{-/-}$ mice. The PI and ROS production were evaluated at different time points after challenge with *Trichophyton rubrum* conidia. The IPR was evaluated 24 hours after cells were challenged with *T. rubrum* conidia. (A) Phagocytic index presented by macrophages from WT and IFN-$\gamma^{-/-}$ mice. (B) IPR of *T. rubrum* conidia inside macrophages of WT compared with the IFN-$\gamma^{-/-}$ group. (C) Kinetics of ROS production by macrophages from WT and IFN-$\gamma^{-/-}$ mice challenged with *T. rubrum* conidia. All groups were tested in triplicate. Results are expressed as the mean ± SEM. $^{**}P < 0.0001$. $^{*}P < 0.05$. IPR, intracellular proliferation rate; WT, wild type.

T. rubrum, since the absence of these cytokines was related to higher fungal burden.

The control of dermatophytosis is related to inflammatory cell migration, predominantly that of neutrophils and macrophages [41], as *T. rubrum* is surrounded by a neutrophilic infiltrate in Majocchi's granuloma [42]. The importance of cell-mediated immunity in the clearance of fungi during dermatophyte infections [40,43] is corroborated by the fact that patients with AIDS may present with relapses of dermatophytosis in which the deep dermal tissue is also involved [42]. Our results show that the amounts of neutrophils and macrophages are correlated with a reduction in fungal burden (Figs 1 and 3). The higher recruitment of neutrophils on the 7th d.p.i., as shown by the MPO activity (Figs 1 and 3), is consistent with the role of these cells in the early stages of the inflammatory response against the infection. However, these cells present lower phagocytic and killing ability compared with that of macrophages, suggesting that neutrophils may act primarily as a producer of chemoattractants to provide the recruitment and activation of macrophages [44–48]. The early recruitment of neutrophils may, in part, be due to the early increases

in TNF-α levels. The rapid increases in IL-1β levels could also support the recruitment of neutrophils to the site of infection by *T. rubrum*, signaled via CXCL1/KC release [28,47]. Conversely, in the later stages of infection, there was lower recovery of fungal cells and lower production of TNF-α and IL-1β and consequently lower neutrophil recruitment. The contribution of the pathway of TNF-α, IL-1β, and CXCL1/KC to the clearance of fungal infections was confirmed in our model; the higher production of these proinflammatory mediators was observed in WT mice and correlated with lower fungal burdens in the skin. The opposite was observed in IL-12- and IFN-γ–deficient mice.

Interestingly, our results showed increased macrophage recruitment in WT mice, suggesting that these cells have a role in controlling the disease (Fig. 1). Activated macrophages are known to execute important antimicrobial activity through the production of ROS [49]. To investigate this phenomenon, we performed a phagocytosis assay. The increased phagocytic index was time dependent in all groups analyzed, and the data confirm the ability of macrophages to contain *T. rubrum* conidia [25]. Cells from IL-12- (data not shown) and IFN-γ–deficient mice presented lower phagocytic indices than cells from WT mice (Fig. 4), suggesting that these two cytokines are important for the activation of macrophages. Although IFN-$\gamma^{-/-}$ mice showed high NAG activity, the *in vitro* experiments demonstrated that the macrophages derived from these animals were not able to prevent *T. rubrum* proliferation due to reduced production of ROS (compared with that of WT mice; Fig. 4). The production of ROS by inflammatory cells is important for microbiocidal activity, and it has been suggested that ROS may be a signal related to inflammasome activation and the production of IL-1β in its active form [16–18,50].

In conclusion, we developed a murine model for dermatophytosis caused by *T. rubrum*, which is an important step in the study of the pathogenesis of this disease. Because the course of this disease is poorly understood, a suitable animal model would increase our understanding of these ringworms. We further demonstrated that IL-12 and IFN-γ are pivotal in the control of *T. rubrum* infection by a mechanism that involves the participation of neutrophils, macrophages, ROS, and IL-1β.

Acknowledgments

This study was supported by the Coordenação de Aperfeiçoamento de Pessoal de Nível Superior (CAPES), Fundação de Amparo à Pesquisa do Estado de Minas Gerais (FAPEMIG), Universidade Federal de Minas Gerais (Programa de Auxílio à Pesquisa de Doutores Recém-Contratados), and Pró-Reitoria de Pesquisa da UFMG. The authors thank Dr Caio Tavares Fagundes and Dr Flávio Amaral for constructive comments.

Declaration of interest

The authors report no conflicts of interest. The authors alone are responsible for the content and the writing of the paper.

References

1. Weitzman I, Summerbell RC. The dermatophytes. *Clin Microbiol Rev* 1995; **8**: 240–259.
2. Vermout S, Tabart J, Baldo A et al. Pathogenesis of dermatophytosis. *Mycopathologia* 2008; **166**: 267–275.
3. Vena GA, Chieco P, Posa F et al. Epidemiology of dermatophytoses: retrospective analysis from 2005 to 2010 and comparison with previous data from 1975. *New Microbiol*; **35**: 207–213.
4. Brand A. Hyphal growth in human fungal pathogens and its role in virulence. *Int J Microbiol*; 2012; **9**: 517–529.
5. Grossman ME, Pappert AS, Garzon MC, Silvers DN. Invasive *Trichophyton rubrum* infection in the immunocompromised host: report of three cases. *J Am Acad Dermatol* 1995; **33**: 315–318.
6. Nir-Paz R, Elinav H, Pierard GE et al. Deep infection by *Trichophyton rubrum* in an immunocompromised patient. *J Clin Microbiol* 2003; **41**: 5298–5301.
7. Sentamilselvi G, Janaki C, Kamalam A, Thambiah AS. Deep dermatophytosis caused by *Trichophyton rubrum*—a case report. *Mycopathologia* 1998; **142**: 9–11.
8. Akiba H, Motoki Y, Satoh M, Iwatsuki K, Kaneko F. Recalcitrant trichophytic granuloma associated with NK-cell deficiency in a SLE patient treated with corticosteroid. *Eur J Dermatol* 2001; **11**: 58–62.
9. Erbagci Z. Deep dermatophytoses in association with atopy and diabetes mellitus: Majocchi's granuloma tricophyticum or dermatophytic pseudomycetoma? *Mycopathologia* 2002; **154**: 163–169.
10. Ashman RB, Vijayan D, Wells CA. IL-12 and related cytokines: function and regulatory implications in *Candida albicans* infection. *Clin Dev Immunol* 2011; **1**: 686–597.
11. Netea MG, Vonk AG, van den Hoven M et al. Differential role of IL-18 and IL-12 in the host defense against disseminated *Candida albicans* infection. *Eur J Immunol* 2003; **33**: 3409–3417.
12. Centeno-Lima S, Silveira H, Casimiro C, Aguiar P, do Rosario VE. Kinetics of cytokine expression in mice with invasive aspergillosis: lethal infection and protection. *FEMS Immunol Med Microbiol* 2002; **32**: 167–173.
13. Chinen T, Qureshi MH, Koguchi Y, Kawakami K. *Candida albicans* suppresses nitric oxide (NO) production by interferon-gamma (IFN-gamma) and lipopolysaccharide (LPS)-stimulated murine peritoneal macrophages. *Clin Exp Immunol* 1999; **115**: 491–497.
14. Kawakami K, Qureshi MH, Zhang T et al. Involvement of endogenously synthesized interleukin (IL)-18 in the protective effects of IL-12 against pulmonary infection with *Cryptococcus neoformans* in mice. *FEMS Immunol Med Microbiol* 2000; **27**: 191–200.
15. Trinchieri G. Interleukin-12 and the regulation of innate resistance and adaptive immunity. *Nat Rev Immunol* 2003; **3**: 133–146.
16. Vonk AG, Netea MG, van Krieken JH et al. Endogenous interleukin (IL)-1 alpha and IL-1 beta are crucial for host defense

against disseminated candidiasis. *J Infect Dis* 2006; **193**: 1419–1426.
17. Schroder K, Tschopp J. The inflammasomes. *Cell* 2010; **140**: 821–832.
18. Dinarello CA. Immunological and inflammatory functions of the interleukin-1 family. *Annu Rev Immunol* 2009; **27**: 519–550.
19. Smijs TG, Bouwstra JA, Schuitmaker HJ, Talebi M, Pavel S. A novel ex vivo skin model to study the susceptibility of the dermatophyte *Trichophyton rubrum* to photodynamic treatment in different growth phases. *J Antimicrob Chemother* 2007; **59**: 433–440.
20. Tabart J, Baldo A, Vermout S et al. Reconstructed interfollicular feline epidermis as a model for *Microsporum canis* dermatophytosis. *J Med Microbiol* 2007; **56**: 971–975.
21. Tani K, Adachi M, Nakamura Y et al. The effect of dermatophytes on cytokine production by human keratinocytes. *Arch Dermatol Res* 2007; **299**: 381–387.
22. Santos DA, Barros ME, Hamdan JS. Establishing a method of inoculum preparation for susceptibility testing of *Trichophyton rubrum* and *Trichophyton mentagrophytes*. *J Clin Microbiol* 2006; **44**: 98–101.
23. Souza DG, Cara DC, Cassali GD et al. Effects of the PAF receptor antagonist UK74505 on local and remote reperfusion injuries following ischemia of the superior mesenteric artery in the rat. *Br J Pharmacol* 2000; **131**: 1800–1808.
24. Barcelos LS, Talvani A, Teixeira AS et al. Impaired inflammatory angiogenesis, but not leukocyte influx, in mice lacking TNFR1. *J Leukoc Biol* 2005; **78**: 352–358.
25. Campos MR, Russo M, Gomes E, Almeida SR. Stimulation, inhibition and death of macrophages infected with *Trichophyton rubrum*. *Microbes Infect* 2006; **8**: 372–379.
26. Oda LM, Kubelka CF, Alviano CS, Travassos LR. Ingestion of yeast forms of *Sporothrix schenckii* by mouse peritoneal macrophages. *Infect Immun* 1983; **39**: 497–504.
27. Ma H, Hagen F, Stekel DJ et al. The fatal fungal outbreak on Vancouver Island is characterized by enhanced intracellular parasitism driven by mitochondrial regulation. *Proc Natl Acad Sci U S A* 2009; **106**: 12980–12985.
28. Amaral FA, Costa VV, Tavares LD et al. NLRP3 inflammasome-mediated neutrophil recruitment and hypernociception depend on leukotriene B(4) in a murine model of gout. *Arthritis Rheum* 2011; **64**: 474–484.
29. Baltazar Lde M, Soares BM, Carneiro HC et al. Photodynamic inhibition of *Trichophyton rubrum*: in vitro activity and the role of oxidative and nitrosative bursts in fungal death. *J Antimicrob Chemother* 2013; **68**: 354–361.
30. Rashid A, Scott E, Richardson MD. Early events in the invasion of the human nail plate by *Trichophyton mentagrophytes*. *Br J Dermatol* 1995; **133**: 932–940.
31. Shimamura T, Kubota N, Shibuya K. Animal model of dermatophytosis. *J Biomed Biotechnol* 2012; **29**: 125–384.
32. Baldo A, Monod M, Mathy A et al. Mechanisms of skin adherence and invasion by dermatophytes. *Mycoses* 2011; **55**: 218–223.
33. Esquenazi D, Alviano CS, de Souza W, Rozental S. The influence of surface carbohydrates during in vitro infection of mammalian cells by the dermatophyte *Trichophyton rubrum*. *Res Microbiol* 2004; **155**: 144–153.
34. Pinzan CF, Ruas LP, Casabona-Fortunato AS, Carvalho FC, Roque-Barreira MC. Immunological basis for the gender differences in murine *Paracoccidioides brasiliensis* infection. *PLoS One* 2010; **5**: e10757.
35. Leal SM, Jr., Vareechon C, Cowden S et al. Fungal antioxidant pathways promote survival against neutrophils during infection. *J Clin Invest* 2012; **122**: 2482–2498.
36. Miyata T, Fujimura T, Masuzawa M, Katsuoka K, Nishiyama S. Local expression of IFN-gamma mRNA in skin lesions of patients with dermatophytosis. *J Dermatol Sci* 1996; **13**: 167–171.
37. Mendez-Tovar LJ. Pathogenesis of dermatophytosis and tinea versicolor. *Clin Dermatol* 2010; **28**: 185–189.
38. Koga T, Ishizaki H, Matsumoto T, Hori Y. In vitro release of interferon-gamma by peripheral blood mononuclear cells of patients with dermatophytosis in response to stimulation with trichophytin. *Br J Dermatol* 1993; **128**: 703–704.
39. Nakamura T, Nishibu A, Yasoshima M et al. Analysis of *Trichophyton* antigen-induced contact hypersensitivity in mouse. *J Dermatol Sci* 2012; **66**: 144–153.
40. Venturini J, Alvares AM, Camargo MR et al. Dermatophyte-host relationship of a murine model of experimental invasive dermatophytosis. *Microbes Infect* 2012; **14**: 1144–1151.
41. Romero FA, Deziel PJ, Razonable RR. Majocchi's granuloma in solid organ transplant recipients. *Transpl Infect Dis* 2011; **13**: 424–432.
42. Smith KJ, Welsh M, Skelton H. *Trichophyton rubrum* showing deep dermal invasion directly from the epidermis in immunosuppressed patients. *Br J Dermatol* 2001; **145**: 344–348.
43. Waldman A, Segal R, Berdicevsky I, Gilhar A. CD4+ and CD8+ T cells mediated direct cytotoxic effect against *Trichophyton rubrum* and *Trichophyton mentagrophytes*. *Int J Dermatol* 2009; **49**: 149–157.
44. Murphy JW. Mechanisms of natural resistance to human pathogenic fungi. *Annu Rev Microbiol* 1991; **45**: 509–538.
45. Bonnett CR, Cornish EJ, Harmsen AG, Burritt JB. Early neutrophil recruitment and aggregation in the murine lung inhibit germination of *Aspergillus fumigatus* conidia. *Infect Immun* 2006; **74**: 6528–6539.
46. Kobayashi SD, DeLeo FR. Role of neutrophils in innate immunity: a systems biology-level approach. *Wiley Interdiscip Rev Syst Biol Med* 2009; **1**: 309–333.
47. Chou RC, Kim ND, Sadik CD et al. Lipid-cytokine-chemokine cascade drives neutrophil recruitment in a murine model of inflammatory arthritis. *Immunity* 2010; **33**: 266–278.
48. Silva MT. When two is better than one: macrophages and neutrophils work in concert in innate immunity as complementary and cooperative partners of a myeloid phagocyte system. *J Leukoc Biol* 2009; **87**: 93–106.
49. Murray PJ, Wynn TA. Protective and pathogenic functions of macrophage subsets. *Nat Rev Immunol* 2011; **11**: 723–737.
50. Gross O, Poeck H, Bscheider M et al. Syk kinase signalling couples to the Nlrp3 inflammasome for anti-fungal host defence. *Nature* 2009; **459**: 433–456.